On the c-Si surface passivation mechanism by the negative-charge-dielectric Al2O3

On the *c*-Si surface passivation mechanism by the negative-charge-dielectric Al_2O_3

B. Hoex,[a] J. J. H. Gielis, M. C. M. van de Sanden, and W. M. M. Kessels[b]
Department of Applied Physics, Eindhoven University of Technology, P.O. Box 513, 5600 MB Eindhoven, The Netherlands

(Received 18 June 2008; accepted 29 September 2008; published online 1 December 2008)

Al_2O_3 is a versatile high-κ dielectric that has excellent surface passivation properties on crystalline Si (*c*-Si), which are of vital importance for devices such as light emitting diodes and high-efficiency solar cells. We demonstrate both experimentally and by simulations that the surface passivation can be related to a satisfactory low interface defect density in combination with a strong field-effect passivation induced by a negative fixed charge density Q_f of up to 10^{13} cm^{-2} present in the Al_2O_3 film at the interface with the underlying Si substrate. The negative polarity of Q_f in Al_2O_3 is especially beneficial for the passivation of *p*-type *c*-Si as the bulk minority carriers are shielded from the *c*-Si surface. As the level of field-effect passivation is shown to scale with Q_f^2, the high Q_f in Al_2O_3 tolerates a higher interface defect density on *c*-Si compared to alternative surface passivation schemes. © *2008 American Institute of Physics*. [DOI: 10.1063/1.3021091]

I. INTRODUCTION

An excellent electrical interface quality is essential for many devices relying on the bulk electronic properties of semiconductors.[1] Electrical losses at a semiconductor interface or surface should be minimized in photonic devices based on group III-V or group IV semiconductors when radiative recombination should be the dominant process.[2,3] In complementary metal-oxide-semiconductor (CMOS) devices, the channel is in direct contact with the interface between the gate dielectric and the semiconductor, and therefore interface defect trapping should be minimized.[4] Moreover, electronic losses at the crystalline Si (*c*-Si) surface have become increasingly important in the field of *c*-Si solar cells due to the trend toward thinner *c*-Si wafers used as base material.[5] Consequently, the reduction of recombination losses at semiconductor interfaces is a prime concern for numerous semiconductor applications.

Recombination losses at a semiconductor interface or surface can be reduced by two different passivation strategies. As the recombination rate is directly proportional to the interface defect density, the first strategy is based on the reduction in the number of defect states at the interface. The interface defect density can be reduced significantly by the passivation of undercoordinated atoms (dangling bonds) by, e.g., atomic H or by a thin dielectric or semiconductor film. This strategy is commonly referred to as chemical passivation. For example, the midgap interface defect density of *c*-Si can be as low as 1×10^9 eV^{-1} cm^{-2} after the growth of a high quality thermal SiO_2 film and a subsequent anneal in a H_2 atmosphere, e.g., a forming gas anneal.[6]

The second strategy to reach surface passivation is based on a significant reduction of the electron or hole concentration at the semiconductor interface by means of a built-in electric field. As recombination processes require both electrons and holes, the highest recombination rate is obtained when the electron and hole concentration at the interface are approximately equal in magnitude (assuming identical capture cross sections for electrons and holes). In other cases the recombination rate scales with the minority carrier concentration at the surface. In the so-called field-effect passivation, the electron or hole concentration at the semiconductor interface is altered by electrostatic shielding of the charge carriers through an internal electric field present at the interface. This internal electric field can either be obtained by a doping profile below the interface or by the presence of fixed electrical charges at the semiconductor interface. Obviously, the principle of field-effect passivation does not apply for CMOS devices such as field effect transistors. A high fixed charge density is even deleterious for the transistor performance as it influences the threshold voltage and the transport of electron and holes in the semiconductor channel.[4,7] Consequently, the application areas of field-effect passivation are limited but the effect can be employed successfully in devices such as light emitting diodes and solar cells.

Recently it was demonstrated that amorphous Al_2O_3 films synthesized by atomic layer deposition (ALD) yield an excellent level of surface passivation on *c*-Si.[8–13] In our previous work, a similar level of surface passivation as state-of-the-art thermal SiO_2 was demonstrated on low resistivity *n*- and *p*-type *c*-Si,[9] whereas highly doped *p*-type Si surfaces were found to be even more effectively passivated by Al_2O_3 than by thermal SiO_2.[10] Remarkably, the Al_2O_3 films, synthesized by plasma-assisted ALD at a substrate temperature of 200 °C, demonstrated no significant level of surface passivation in the *as-deposited* state.[9,10] A 30 min postdeposition anneal at 425 °C in N_2 was required to obtain the level of surface passivation reported. A nonspecified thermal treatment was also required for an optimal level of surface passivation in the study of Agostinelli *et al.* for Al_2O_3 films

[a]Current address: Solar Energy Research Institute Singapore, National University of Singapore, Block E4-01-01, Singapore 117576, Singapore. Electronic mail: bram.hoex@gmail.com.
[b]Electronic mail: w.m.m.kessels@tue.nl.

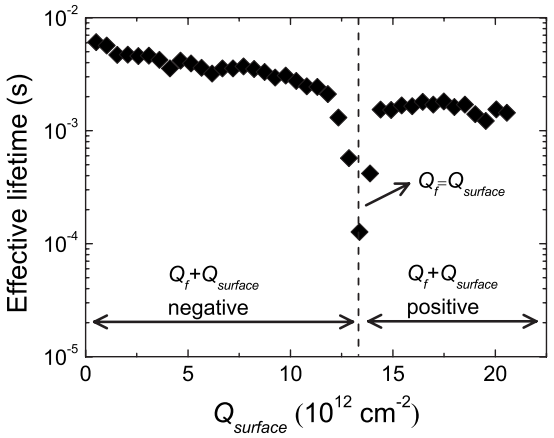

FIG. 1. Effective lifetime of a 1.9 Ω cm *n*-type *c*-Si wafer passivated on both sides by a 26 nm thick Al_2O_3 film. The effective lifetime is presented as a function of the positive charge density $Q_{surface}$ deposited at the Al_2O_3 on one side of the wafer in a corona charging experiment. Field-effect passivation is ruled by the sum of the negative fixed charge density Q_f in the Al_2O_3 film and the positive $Q_{surface}$. The effective lifetime was determined at an injection level of $10^{14}-10^{15}$ cm^{-3}.

synthesized by thermal ALD.[8] The excellent level of surface passivation that can be achieved by ALD-synthesized Al_2O_3 films was recently also confirmed at the device level. Al_2O_3 applied at the rear of a diffused emitter *p*-type *c*-Si solar cells yielded a conversion efficiency of 20.6%,[12] and Al_2O_3 applied at the front side *p*-type emitter of *n*-type solar cells yielded a conversion efficiency of 23.2%.[13]

In this paper, we will address the underlying mechanism of *c*-Si surface passivation as obtained by amorphous Al_2O_3 films. From results obtained on Al_2O_3 films synthesized by plasma-assisted ALD, it will be demonstrated that in addition to a satisfactory low interface defect density, the surface passivation is ruled for a large part by a strong field-effect passivation induced by a relatively high negative fixed charge density Q_f in the Al_2O_3 film. On the basis of simulations, it will be discussed that the field-effect passivation scales with Q_f^2 and, consequently, the high Q_f in Al_2O_3 tolerates a higher interface defect density than other passivation films with lower Q_f values. It will be shown that the postdeposition anneal increases the negative Q_f and lowers the interface defect density of the $Si/SiO_x/Al_2O_3$ system resulting in a significant improvement of the level of surface passivation obtained. The presence of an interfacial SiO_x film between *c*-Si and the Al_2O_3 appears to play a key role in both the origin of the negative Q_f and the interface defect density. As a negative Q_f in combination with a sufficiently low interface defect density is routinely reported for Al_2O_3 films deposited on *c*-Si, irrespective of the deposition technique, it is argued that the findings presented in this paper are not limited to Al_2O_3 films synthesized by (plasma-assisted) ALD.

II. Al_2O_3 AS NEGATIVE CHARGE DIELECTRIC

The field-effect passivation of *c*-Si by Al_2O_3 is experimentally demonstrated in Fig. 1. A high quality 1.9 Ω cm *n*-type *c*-Si wafer with a thickness of 275 μm was passivated on both sides by a 26 nm thick Al_2O_3 film synthesized by plasma-assisted ALD.[11] The resulting effective lifetime of the passivated *c*-Si wafer exceeds 6 ms indicating that the *c*-Si surfaces are adequately passivated by Al_2O_3. Subsequently a positive charge density $Q_{surface}$ is applied at the Al_2O_3 surface in a corona charging experiment. In this case, the field-effect passivation is ruled by the sum of Q_f and $Q_{surface}$. From the figure, it is clear that a positive $Q_{surface}$ up to 10^{13} cm^{-2} hardly affects the effective lifetime of the *c*-Si wafer. However, a positive $Q_{surface}$ in the range of $(1.2-1.4)\times10^{13}$ cm^{-2} leads to a strong decrease in the effective lifetime. A minimum effective lifetime of ~100 μs is obtained for a positive $Q_{surface}$ of 1.3×10^{13} cm^{-2}. At this stage, the positive $Q_{surface}$ balances the negative Q_f in the Al_2O_3 film, which nullifies the level of field-effect passivation.[11] For a positive $Q_{surface}$ exceeding the amount of negative Q_f [$Q_{surface}$ in the range of $(1.3-2.0)\times10^{13}$ cm^{-2}] field-effect passivation is provided by the positive charge density at the *c*-Si surface. Summarizing, Fig. 1 clearly demonstrates the mechanism of field-effect passivation on *c*-Si, and it reveals that the negative Q_f in this 26 nm thick Al_2O_3 film is $(1.3\pm0.1)\times10^{13}$ cm^{-2}.

Al_2O_3 has extensively been investigated for the application as gate and charge trapping dielectric on *c*-Si where also high negative Q_f values have been reported. For gate dielectric applications in CMOS, a low interface defect density and a low Q_f are essential,[4] whereas a low interface defect density in combination with a high density of electronically active bulk defects is desired for charge trapping dielectrics such as applied in nonvolatile memory.[14,15] Table I summarizes the bulk and interface electronic properties reported in the literature for Al_2O_3 films deposited on *c*-Si by various techniques. The sign of Q_f is always negative for the Al_2O_3 films after annealing, irrespective of the deposition technique.[16] The magnitude of Q_f is typically in the range of $10^{12}-10^{13}$ cm^{-2} for annealed Al_2O_3 films, in good agreement with our results in Fig. 1. From thickness dependent capacitance-voltage measurements, it was deduced that the negative Q_f is independent of the Al_2O_3 thickness and is located at the interface with the substrate.[17–19]

It is interesting to note that negative fixed charges are detected in Al_2O_3 films deposited on H-terminated *c*-Si as well as Al_2O_3 films deposited on *c*-Si covered by a 1–100 nm thick SiO_2 film. Despite the fact that Al_2O_3 is thermodynamically stable on *c*-Si, Al_2O_3 deposition processes occur under nonequilibrium conditions, and as a result an interfacial SiO_x layer is commonly formed between the Al_2O_3 film and the *c*-Si substrate.[20–23] This SiO_x layer can be formed during the Al_2O_3 deposition process but also during the postdeposition annealing treatment. The unintentional formation of an interfacial SiO_x is undesired for the application of Al_2O_3 as gate dielectric in CMOS devices as it lowers the effective dielectric constant of the layer stack. Nevertheless, only a very limited number of studies (e.g., in the work of Gusev *et al.*[24]) report on the absence of an interfacial SiO_x layer between the Al_2O_3 film and *c*-Si substrate.[4] An interfacial SiO_x film was also detected by high resolution transmission electron microscopy (HR-TEM) in the Al_2O_3 films synthesized by plasma-assisted ALD, both in the as-deposited and annealed state, that demonstrated an excellent level of surface passivation on *c*-Si.[9]

TABLE I. Bulk and interface electronic properties for Al_2O_3 films deposited on *c*-Si as reported in the literature. All films were deposited on H-terminated *c*-Si unless indicated otherwise. In all cases, Q_f was extracted from the flatband voltage shift determined from capacitance-voltage (*CV*) measurements of MOS structures. The interface defect density was extracted from *CV* and/or conductance measurements of MOS structures. Most samples were analyzed after a postdeposition anneal, however, some samples were also measured as-deposited (indicated with "a–d").

Negative Q_f (10^{12} cm^{-2})	D_{it} at midgap (10^{11} eV^{-1} cm^{-2})	Deposition method	Deposition temperature (°C)	Postdeposition thermal treatment	Ref.
0.2–0.5	···	Pyrolysis of $Al(C_3H_8O)_3$ on *c*-Si with 23–100 nm thermal SiO_2	425	30 min FGA[a] at 425 °C	17
0.2–0.5	···	CVD from $AlBr_3$+NO on *c*-Si with 23–100 nm thermal SiO_2	910	30 min FGA[a] at 425 °C	17
−0.5 (a–d)	15 (a–d)	Pyrolysis of $Al(C_3H_8O)_3$ on *c*-Si			
3.2	0.8	with 1.5 nm native SiO_2	360	15 min FGA[a] at 510 °C	39
10–11 (a–d)	···	Pyrolysis of $AlCl_3$ in CO_2/H_2 environment[b]	900	None	15
0.6 (a–d)	~1	ALD from $Al(CH_3)+H_2O$	450	None	48
~2	0.8	ALD from $Al(CH_3)_3$ and H_2O	350	Various at 585 °C and 800 °C	49
···	0.3	Oxidation of evaporated Al	<400	800 °C in N_2	50
7	1–3	ALD from $AlCl_3$ and H_2O [c]	370	None	19
7 (a–d)	13 (a–d)			FGA[a] at 300–450 °C and	
6–7	1	ALD from $Al(CH_3)_3$ and H_2O [b]	350	anneal in N_2 at 450 °C	46
5–10 (a–d)	2–5[d] (a–d)	Reactive target sputtering in Ar/O_2	380	FGA[a]	51
···	2–10 (a–d)	ALD from $AlCl_3$ and H_2O	300–800	None	52
···	20	ALD from $Al(CH_3)_3$ and H_2O	300	30 min FGA[a] at 400 °C	53
13[e](a–d)					
6[e]	···	ALD from $Al(CH_3)_3$ and O_3	400	None or 10 min at 800 °C in N_2	54
		Molecular beam epitaxy from Al and N_2O on *c*-Si with an interfacial layer		None or anneal at 600 °C	
3–9	···	formed from Al and chemical SiO_2[f]	750	in O_2, N_2, H_2 or air	55
3–8 (a–d)	···	ALD from $Al(CH_3)_3$ and H_2O on *c*-Si with 7 nm thermal SiO_2	160–350	None	56
Up to 10	···	ALD from $Al(CH_3)_3$ and H_2O [b]	<300	Yes, not specified	8
		Remote plasma enhanced CVD from metal		30 s anneal at 800 °C and	
7	···	organic[g] and O_2 on *c*-Si [h]	300	30 min FGA[a] at 425 °C	18
0.2–2 (a–d)					
5–8		ALD from $Al(CH_3)_3$ and O_2 plasma	200	30 min anneal at 425 °C	44

[a]Forming gas anneal, typically 5%–10% H_2 in N_2.
[b]The pretreatment of the *c*-Si wafer was not specified.
[c]The defect density could be lowered by the addition of Zr or Si in the Al_2O_3 to values in the mid 10^{10} eV^{-1} cm^{-2} range.
[d]The Al_2O_3 films were grown under UV radiation.
[e]The Al_2O_3 film was covered with a HfO_2 film.
[f]Polycrystalline Al_2O_3 was grown in this study due to epitaxy process.
[g]$(CH_2)_3Al_2(C_4H_9O)_3$
[h]Films were grown at H-terminated *c*-Si and *c*-Si with 1.0 or 1.6 nm thermal SiO_2 with no significant impact on the amount of negative Q_f.

The origin of the negative Q_f in Al_2O_3 deposited on *c*-Si has been attributed to intrinsic and extrinsic defects in Al_2O_3. Matsunaga *et al.* calculated the energetics of intrinsic vacancies and interstitials in Al_2O_3 from first principles.[25] These calculations showed that each intrinsic point defect is most stable in their fully ionized form. Hence, Al vacancies and O interstitials exhibit a negative charge and Al interstitials and O vacancies exhibit a positive charge in good agreement with the ionic nature of the Al_2O_3.[25] Extrinsic H has also been proposed as origin for the negative fixed charges in Al_2O_3. Peacock and Robertson calculated that interstitial H acts as a deep trap site for electrons in Al_2O_3.[26] H is, for example, a common constituent in Al_2O_3 synthesized by ALD because H-containing precursors such as $Al(CH_3)_3$ and H_2O are used in the deposition process. Hence, Al vacancies, O interstitials, and interstitial H are proposed as the origin of the negative Q_f in Al_2O_3. Based on the ionic nature of Al_2O_3, Lucovsky postulated that Al_2O_3 consists of tetrahedrally coordinated Al in AlO_4^- units and octahedrally coordinated Al^{3+} in a ratio of 3:1 to assure charge neutrality.[27] Kimoto *et al.* demonstrated that both tetrahedrally and octahedrally coordinated Al are present in Al_2O_3 grown by thermal ALD on H-terminated *c*-Si.[28] However, tetrahedrally coordinated Al was found to be dominant at the interface. This dominance was attributed to the fact that Si in the interfacial SiO_x film also has a tetrahedral coordination.[28] Consequently, the interfacial SiO_x film could fulfill an important role in the origin of the negative Q_f that is found in Al_2O_3 films grown on *c*-Si by inducing a high density of negatively charged Al vacancies close to the interface. This hypothesis is in good agreement with the location of the negative Q_f extracted from thickness dependent *CV* measurements by various authors.[17–19]

The polarity of Q_f plays an important role in the surface passivation of *c*-Si. The most commonly used dielectric passivation films on *c*-Si, i.e., thermal SiO_2, *a*-SiC_x:H, and *a*-SiN_x:H contain a positive Q_f and lead to a high level of surface passivation of lightly doped *n*- and *p*-type *c*-Si and

highly doped *n*-type *c*-Si surfaces.[29–31] A positive Q_f has, however, been shown to be detrimental for the passivation of highly *p*-type surfaces such as in *p*-type emitters on *n*-type solar cells because the minority electrons are attracted to the *c*-Si surface and thereby enhance the recombination rate.[10] Positive-charge dielectrics also demonstrate a strong injection level dependence for the surface passivation properties on lightly doped *p*-type *c*-Si.[31–33] The level of surface passivation decreases when going to lower excess carrier concentrations (i.e., lower injection levels), which is, for example, detrimental for the *c*-Si solar cell efficiency under low illumination conditions.[29] This injection level dependence is attributed to additional bulk recombination losses in the inversion layer close to the *c*-Si surface.[34] The inversion layer is created by the shielding of holes, which are the majority carriers in the *p*-type *c*-Si bulk, from the *c*-Si surface by the positive Q_f in the dielectric film. For the negative-charge dielectric Al_2O_3 on the other hand, it has been demonstrated that the level of surface passivation is constant at low injection level for lightly doped *p*-type *c*-Si.[9] On the contrary, when the negative-charge dielectric Al_2O_3 is used to passivate lightly doped *n*-type *c*-Si, the level of surface passivation decreases when going to lower injection level,[9] whereas positive-charge dielectrics demonstrate a constant level of surface passivation in this case.[32,33] Hence, a similar bulk recombination in the inversion layer could explain this injection level behavior of lightly doped *n*-type *c*-Si passivated by the negative-charge dielectric Al_2O_3. Furthermore, the high positive Q_f in *a*-SiN_x:H causes the so-called parasitic shunting effect when applied at the rear of *p*-type *c*-Si solar cells and thereby significantly decreases the short-circuit current of *c*-Si solar cells.[35] This effect is absent when the negative-charge dielectric Al_2O_3 is used at the rear of diffused front side emitter *p*-type *c*-Si solar cells, which has resulted in solar cell efficiencies of 20.6%.[12] The negative charge in Al_2O_3 is even more important in the passivation of highly doped *p*-type *c*-Si surfaces as the shielding of the minority carriers, the electrons, from the surface by the negative charges leads to a much higher level of passivation than positive-charge dielectrics such as thermal SiO_2 and as-deposited *a*-SiN_x:H.[10] The latter was recently also demonstrated at the device level by an exceptionally high conversion efficiency of 23.2% obtained for an *n*-type solar cell with a front side B-doped *p*-type emitter passivated by a 30 nm thick Al_2O_3 film.[13]

III. FIELD EFFECT PASSIVATION VERSUS CHEMICAL PASSIVATION

It is evident that besides the polarity of the fixed charge, the amount of fixed charge is also important for field-effect passivation. Figure 2 shows the effective surface recombination velocity S_{eff} at an injection level of 5×10^{14} cm^{-3} (corresponding to approximately 1 sun illumination) as a function of the negative Q_f located at the surface for moderately doped *n*-type ($[\text{P}]=7\times10^{15}$ cm^{-3}) and *p*-type ($[\text{B}]=7\times10^{15}$ cm^{-3}) *c*-Si. The simulations were performed using the extended Shockley–Read–Hall model as proposed by Girisch *et al.*[36] The fundamental recombination velocities of

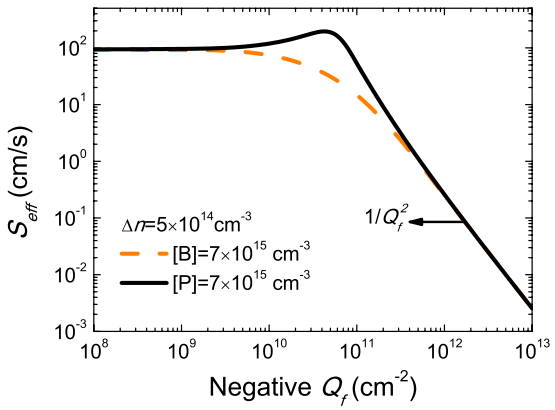

FIG. 2. (Color online) Simulated effective surface recombination velocity S_{eff} at an injection level Δn of 5×10^{14} cm^{-3} for moderately doped *n*-type ($[\text{P}]=7\times10^{15}$ cm^{-3}) and *p*-type ($[\text{B}]=7\times10^{15}$ cm^{-3}) *c*-Si as a function of the negative Q_f located at the *c*-Si surface.

the electrons and holes were taken to be energy independent and equal to 100 cm/s. Figure 2 clearly shows that a negative Q_f decreases the S_{eff} at a *p*-type *c*-Si surface. On the other hand, Fig. 2 demonstrates that a relatively small negative Q_f up to 5×10^{10} cm^{-2} increases the S_{eff} for moderately doped *n*-type *c*-Si. For higher negative Q_f values, the S_{eff} decreases for *n*-type *c*-Si, and for a negative $Q_f>3\times10^{11}$ cm^{-2} the S_{eff} is practically equal for *n*- and *p*-type *c*-Si. As already mentioned, the surface recombination rate is proportional to the minority carrier concentration at the surface. For a negative Q_f in the range of $5\times10^{10}-1\times10^{13}$ cm^{-2}, electrons are the minority carriers at the surface of both *n*- and *p*-type *c*-Si. The increasing S_{eff} for *n*-type *c*-Si up to a negative Q_f of 5×10^{10} cm^{-2} can be explained by the fact that for this low negative Q_f holes are still the minority carrier at the *n*-type *c*-Si surface and the hole concentration, hence the recombination, is increased by electrostatic interaction by the presence of the negative charge at the surface. A similar effect can be observed for *p*-type *c*-Si passivated by positive charge dielectrics as was shown by Aberle *et al.*[29] For negative $Q_f>5\times10^{11}$ cm^{-2}, S_{eff} scales with $1/Q_f^2$ for both *n*- and *p*-type *c*-Si. This is in good agreement with the results reported by Kuhlmann *et al.* for inverted *p*-type *c*-Si surfaces.[37]

The Q_f^2 dependence of the field-effect passivation allows us to compare the relative strength of field-effect passivation by Al_2O_3 and other charge containing dielectrics used for *c*-Si surface passivation. For thermal SiO_2 and *a*-SiC_x:H, a relatively low positive Q_f around 10^{11} cm^{-2} on *p*-type *c*-Si is commonly reported,[29,31,34] whereas for *a*-SiN_x:H, a positive Q_f in the range of 10^{12} cm^{-2} is typically found.[38–40] Consequently, the field-effect passivation provided by Al_2O_3 is up to four orders of magnitude stronger compared to thermal SiO_2 and *a*-SiC_x:H and up to two orders of magnitude stronger compared to *a*-SiN_x:H.

Besides field-effect passivation, chemical passivation also reduces the recombination losses at *c*-Si surfaces. For example, the state-of-the-art surface passivation by thermal SiO_2 can mainly be attributed to chemical passivation due to its extremely low interface defect density. A strong field-effect passivation as in the case of Al_2O_3, however, relaxes

the requirements on the interface defect density. Using the Q_f^2 scaling of the field-effect passivation, we can estimate the relative importance of the chemical passivation for Al_2O_3 compared to thermal SiO_2 for lightly doped *c*-Si. Assuming similar electron and hole capture cross sections for the dominant defects, the midgap defect density at the *c*-Si surface is allowed to be as high as 10^{13} eV^{-1} cm^{-2} to yield a similar level of surface passivation compared to thermal SiO_2 with a midgap interface defect density of 10^9 eV^{-1} cm^{-2}.[6] However, from Fig. 1, it can be concluded that the Al_2O_3 film with the interfacial SiO_x film also provides a good level of chemical passivation because the effective lifetime is still relative high at ~100 μs when the negative Q_f in the Al_2O_3 film is balanced (for a poorly passivated surface the effective lifetime would only be ~5 μs). Hence, the interface defect density between the Al_2O_3/SiO_x film and the *c*-Si substrate is expected to be reasonably low. As can be seen in Table I, typically interface defect densities in the range of 10^{11} eV^{-1} cm^{-2} have been reported for annealed Al_2O_3 films on *c*-Si, which is up to two orders of magnitude higher compared to thermal SiO_2. Similar to thermal SiO_2, the lowest interface defect density is obtained by postdeposition annealing treatments, either an anneal in a H_2 containing atmosphere in the 300–500 °C temperature range or a short high temperature anneal in N_2 below the crystallization temperature of Al_2O_3. Moreover, the interface defect density of dielectrics on *c*-Si has *empirically* been related to the average bonding concentration at the interface by Lucovsky *et al.*[41] Dielectrics with an average bonding concentration above 3 would exhibit a high interface defect density and vice versa. As the average bonding concentration of Al_2O_3 is 3.6, the interface defect density at the *c*-Si surface could be significantly lowered by the presence of a thin SiO_2-like film between the *c*-Si and the Al_2O_3 because SiO_2 has an average bonding density of 2.8.[41]

The interface defect density is also of relevance due to the fact that interface defect states can trap charges and thereby could potentially cancel part of the field-effect passivation provided by the Q_f in the passivation film. The influence of the charging of interface defect states on the surface passivation of *a*-Si:H on *c*-Si has been reported by Garin *et al.*[42] and Obilet *et al.*[43] Nevertheless, the effect of trapped charges becomes only of significance when the interface defect density is of the same order as Q_f. Hence, for Al_2O_3 on *c*-Si, it is not expected that this effect can be significant because the defect densities are typically at least one order of magnitude lower than the magnitude of the negative Q_f in the film (see Table I).

As mentioned, Al_2O_3 synthesized by plasma-assisted ALD provides no significant level of surface passivation of *c*-Si in the as-deposited state, whereas the level of surface passivation is excellent after a 30 min anneal at 425 °C in N_2.[9,10] This difference in surface passivation performance of the Al_2O_3 can partly be related to changes in the negative fixed charge density Q_f after annealing. In Fig. 3, the effective lifetime for *c*-Si wafers is shown for Al_2O_3 films with a thickness between 6 and 32 nm in the as-deposited and annealed state. The films were deposited on both sides of 275 μm 1.9 Ω cm *n*-type *c*-Si wafers by plasma-assisted

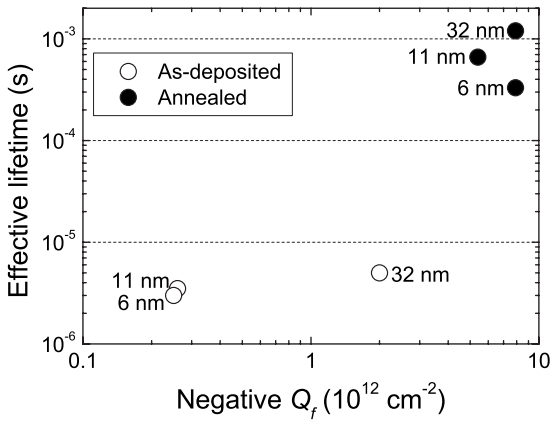

FIG. 3. Measured effective lifetime at an injection level of 5×10^{14} cm^{-3} of a 275 μm 1.9 Ω cm *n*-type *c*-Si wafer passivated on both sides by a 6, 11, and 32 nm thick Al_2O_3 film plotted as a function of the measured negative Q_f in the Al_2O_3 film. Q_f and the effective lifetime were determined for the as-deposited films and after a subsequent 30 min postdeposition anneal at 425 °C in N_2.

ALD at a substrate temperature of 200 °C.[9] The Q_f in the Al_2O_3 films was determined by the contactless optical second-harmonic generation technique (as described in detail in a separate publication[44]), and the effective lifetime was determined by the contactless photoconductance technique The as-deposited Al_2O_3 films already contain a negative Q_f in the range of $(3-20)\times10^{11}$ cm^{-2} without demonstrating any level of surface passivation as indicated by the low effective lifetime in the range of 3–5 μs. After annealing, the negative Q_f has increased for all films and is within the range of $(5-8)\times10^{12}$ cm^{-2}. The effective lifetime also increases over more than two orders of magnitude and reaches a value of 1.2 ms for *c*-Si wafer passivated by the 32 nm thick Al_2O_3 film. Capacitance-voltage (*CV*) analysis also confirmed the increase in negative Q_f after the postdeposition anneal.[11] It should also be noted that the negative Q_f in the as-deposited 32 nm Al_2O_3 film of 2×10^{12} cm^{-2} is significantly higher compared to the negative Q_f of $\sim3\times10^{11}$ cm^{-2} that is found in the as-deposited 6 and 11 nm thick Al_2O_3 films. This is possibly related to the significant longer deposition time of the 32 nm Al_2O_3 film, which leads to an annealing effect during the deposition process itself. The difference in effective lifetime between the annealed 11 and 32 nm Al_2O_3 film scales with Q_f^2 and can consequently be attributed to a difference in field-effect passivation. On the other hand, the relative low effective lifetime of the *c*-Si wafer passivated by the annealed 6 nm thick film indicates a lower chemical passivation and consequently a higher interface defect density compared to the annealed 11 and 32 nm thick Al_2O_3 films.

Using the Q_f^2 scaling of the field-effect passivation, it can be argued that the increase in Q_f of the 32 nm Al_2O_3 film only leads in an increase in the level of field-effect passivation by a factor 16 compared to the Al_2O_3 film in the as-deposited state, while the effective lifetime actually increases by more than two orders of magnitude. Consequently the important conclusion can be drawn that the postdeposition anneal also improves the chemical passivation of the 32 nm thick Al_2O_3 film by a reduction of the interface defect density. As a matter of fact, the low effective lifetime in combi-

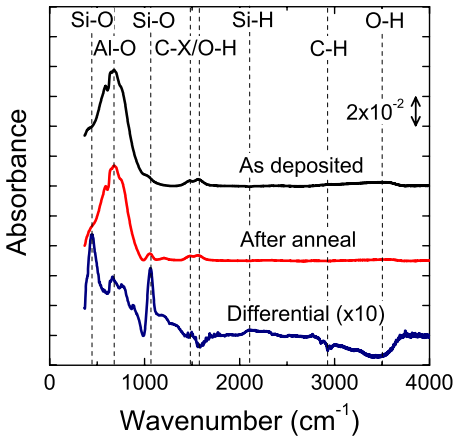

FIG. 4. (Color online) Infrared absorption spectra of a 30 nm thick Al_2O_3 film, which was synthesized by plasma-assisted ALD on both sides of a high resistivity *c*-Si substrate. Data is presented in the as-deposited and annealed state. Absorption peaks related to Al–O, Si–O, C–H, O–H, and Si–H bonds can clearly be distinguished in the spectra as indicated. For clarity, the differential absorption spectrum is also shown indicating the changes in the Al_2O_3 resulting from the postdeposition anneal (positive and negative peaks with respect to the baseline correspond to the appearance and disappearance of absorbing species).

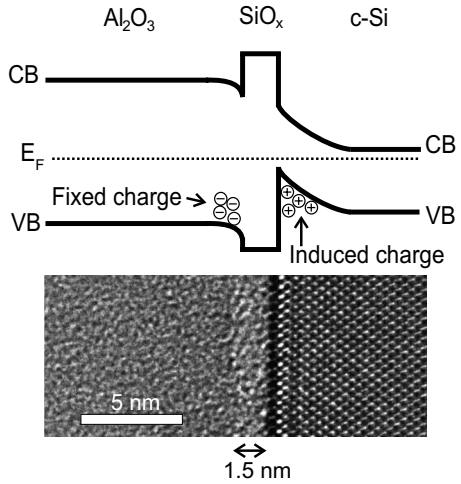

FIG. 5. Schematic band diagram of the *n*-type *c*-Si/SiO_x/Al_2O_3 system (VB denotes valence band energy, CB denotes conduction band energy, and E_F denotes Fermi energy). The HR-TEM image shows the *c*-Si/SiO_x/Al_2O_3 interface (the black line between the SiO_x and *c*-Si is a TEM artifact). A high negative Q_f is present in the Al_2O_3 film at the Al_2O_3/SiO_x interface effectively shields electrons from the *c*-Si surface. A relative good interface quality is assured by the presence of a thin interfacial SiO_x film between the *c*-Si substrate and the Al_2O_3 film.

nation with a relative high fixed charge density of 2×10^{12} cm^{-2} for the *c*-Si wafer passivated by the as-deposited 32 nm Al_2O_3 film clearly demonstrates that chemical passivation plays a very important role in the surface passivation mechanism of the annealed Al_2O_3 films. The reduction of the interface defect density between the Al_2O_3 film and the *c*-Si substrate after the postdeposition annealing treatment was also confirmed by *CV* measurements, which showed a significant decrease in the parallel conductance.[45] It should be noted that a postdeposition anneal is routinely employed to improve the electrical quality of the interface between *c*-Si and dielectric films. This was also demonstrated for the *c*-Si/Al_2O_3 system in the studies of Hezel and Jaeger[39] and Jeon *et al.*[46] In both studies, the *c*-Si/Al_2O_3 interface defect density was lowered over more than one order of magnitude (down to $\sim 1 \times 10^{11}$ eV^{-1} cm^{-2}) by a postdeposition annealing step similar to the anneal applied to the Al_2O_3 films in Fig. 3.

Other than changes in the bulk and interface electronic properties, structural changes in the *c*-Si/Al_2O_3 system are also commonly reported after a postdeposition anneal.[20,23] These structural changes are possibly related to the changes in the Al_2O_3 bulk and interface electronic properties. HR-TEM revealed the presence of an interfacial oxide layer between the amorphous Al_2O_3 film synthesized by plasma-assisted ALD and the *c*-Si substrate and this layer slightly increased in thickness from 1.2 nm in the as-deposited state to 1.5 nm after a postdeposition anneal.[9] This interfacial oxide layer consists of SiO_x and the presence of Si–O bonds is confirmed by infrared absorbance spectra of as-deposited and annealed Al_2O_3 films, as shown in Fig. 4. Particularly after the postdeposition anneal, the Si–O absorption peak in the infrared absorbance spectrum is very similar to the absorption peak observed for good quality thermal SiO_2.[47] Chowdhuri *et al.*[20] and Kuse *et al.*[23] also showed a strong increase in Si–O related absorption by infrared spectroscopy and x-ray photoelectron spectroscopy after annealing ALD-synthesized Al_2O_3 films on *c*-Si.[20,23] As the absorption intensity of both Si–O and Al–O bonds increase after the postdeposition anneal, it can be argued that the increase in interfacial oxide thickness by TEM can mainly be attributed to a restructuring in the interfacial oxide instead of an additional oxidation of the underlying *c*-Si substrate. As mentioned, the interfacial SiO_x film could play an important role in the origin of the negative Q_f in the Al_2O_3 film, and hence the changes in the Si–O related absorption could correlate with the change in the magnitude of the negative Q_f in the Al_2O_3 film. The infrared absorbance spectrum in Fig. 4 also confirms the presence of H in the form of O–H groups in the Al_2O_3 film. The O–H density decreases after the postdeposition anneal and this decrease coincides with the formation of both Al–O and Si–O bonds. The H atoms released during the anneal can passivate Si dangling bond defects states at the interface as corroborated by an increase in Si–H related absorbance.

IV. CONCLUSIONS

To summarize, it has been demonstrated that the excellent surface passivation of *c*-Si by Al_2O_3 films synthesized by plasma-assisted ALD can be explained by a satisfactory low interface defect density in combination with a very high negative Q_f in the Al_2O_3 film. As schematically illustrated in Fig. 5, a high negative Q_f strongly reduces the electron concentration at the *c*-Si interface by means of electrostatic shielding. The negative charges are localized in the Al_2O_3 film close to the interface with the *c*-Si substrate that is separated from the Al_2O_3 through an interfacial SiO_x layer. The charges most likely originate from Al vacancies resulting from a preferential tetrahedral coordination of Al in the region close to the interfacial SiO_x. The unique negative polarity of Q_f is especially beneficial for the passivation of *p*-type *c*-Si, including *p*-type emitters on *n*-type solar cells, as the bulk minority carriers are shielded from the *c*-Si surface.

When the negative Q_f in the Al_2O_3 film is balanced by a positive $Q_{surface}$, still some level of chemical passivation is provided indicating that the interface defect density is also relatively low. The significant improvement in the level of *c*-Si surface passivation by Al_2O_3 after a postdeposition anneal can be related to changes in both surface passivating mechanisms, i.e., the negative Q_f significantly increases and the interface defect density decreases as indicated by the higher quality interfacial SiO_x. It has also been addressed that a high negative charge density Q_f tolerates a relatively high defect density at the *c*-Si interface while maintaining a good level of surface passivation. Because high negative Q_f values are routinely reported for Al_2O_3 films deposited on *c*-Si, irrespective of the deposition technique, it appears that the bulk and interface electrical quality required for excellent surface passivation of *c*-Si are not limited to Al_2O_3 films synthesized by ALD but are accessible for a broad range of deposition techniques.

ACKNOWLEDGMENTS

The authors thank W. Keuning, J. L. van Hemmen, M. J. F. van de Sande, J. F. C. Jansen, and J. J. A. Zeebregts for their technical assistance and their help during the experiments. Dr. I. Martin (Universitat Politecnica de Catalunya) and Dr. J. Schmidt (Institut für Solarenergieforschung Hameln/Emmerthal) are acknowledged for the fruitful discussions on the lifetime data. This work is supported by the Netherlands Technology Foundation STW. The work of B.H. is supported by OTB Solar.

[1] H. J. Queisser and E. E. Haller, Science **281**, 945 (1998).
[2] M. Boroditsky, I. Gontijo, M. Jackson, R. Vrijen, E. Yablonovitch, T. Krauss, C. C. Cheng, A. Scherer, R. Bhat, and M. Krames, J. Appl. Phys. **87**, 3497 (2000).
[3] M. J. Chen, Y. T. Shih, M. K. Wu, and F. Y. Tsai, J. Appl. Phys. **101**, 033130 (2007).
[4] G. D. Wilk, R. M. Wallace, and J. M. Anthony, J. Appl. Phys. **89**, 5243 (2001).
[5] A. G. Aberle, Prog. Photovoltaics **8**, 473 (2000).
[6] H. Jin, K. J. Weber, N. C. Dang, and W. E. Jellett, Appl. Phys. Lett. **90**, 262109 (2007).
[7] G. Lucovsky, J. Vac. Sci. Technol. A **19**, 1553 (2001).
[8] G. Agostinelli, A. Delabie, P. Vitanov, Z. Alexieva, H. F. W. Dekkers, S. De Wolf, and G. Beaucarne, Sol. Energy Mater. Sol. Cells **90**, 3438 (2006).
[9] B. Hoex, S. B. S. Heil, E. Langereis, M. C. M. van de Sanden, and W. M. M. Kessels, Appl. Phys. Lett. **89**, 042112 (2006).
[10] B. Hoex, J. Schmidt, R. Bock, P. P. Altermatt, M. C. M. van de Sanden, and W. M. M. Kessels, Appl. Phys. Lett. **91**, 112107 (2007).
[11] B. Hoex, J. Schmidt, P. Pohl, M. C. M. van de Sanden, and W. M. M. Kessels, J. Appl. Phys. **104**, 044903 (2008).
[12] J. Schmidt, A. Merkle, R. Brendel, B. Hoex, M. C. M. van de Sanden, and W. M. M. Kessels, Prog. Photovoltaics **16**, 461 (2008).
[13] J. Benick, B. Hoex, M. C. M. van de Sanden, W. M. M. Kessels, O. Schultz, and S. Glunz, Appl. Phys. Lett. **92**, 253504 (2008).
[14] M. Specht, H. Reisinger, F. Hofmann, T. Schulz, E. Landgraf, R. J. Luyken, W. Rosner, M. Grieb, and L. Risch, Solid-State Electron. **49**, 716 (2005).
[15] D. A. Mehta, S. R. Butler, and F. J. Feigl, J. Appl. Phys. **43**, 4631 (1972).
[16] In the studies of Chin *et al.* (Ref. 50) and Duenas *et al.* (Ref. 52) also positive flatband voltage shifts were reported indicating a negative fixed charge density.
[17] J. A. Aboaf, D. R. Kerr, and E. Bassous, J. Electrochem. Soc. **120**, 1103 (1973).
[18] R. S. Johnson, G. Lucovsky, and I. Baumvol, J. Vac. Sci. Technol. A **19**, 1353 (2001).
[19] S. Y. No, D. Eom, C. S. Hwang, and H. J. Kim, J. Electrochem. Soc. **153**, F87 (2006).
[20] A. Roy Chowdhuri, C. G. Takoudis, R. F. Klie, and N. D. Browning, Appl. Phys. Lett. **80**, 4241 (2002).
[21] S. C. Ha, E. Choi, S. H. Kim, and J. S. Roh, Thin Solid Films **476**, 252 (2005).
[22] R. F. Klie, N. D. Browning, A. R. Chowdhuri, and C. G. Takoudis, Appl. Phys. Lett. **83**, 1187 (2003).
[23] R. Kuse, M. Kundu, T. Yasuda, N. Miyata, and A. Toriumi, J. Appl. Phys. **94**, 6411 (2003).
[24] E. P. Gusev, M. Copel, E. Cartier, I. J. R. Baumvol, C. Krug, and M. A. Gribelyuk, Appl. Phys. Lett. **76**, 176 (2000).
[25] K. Matsunaga, T. Tanaka, T. Yamamoto, and Y. Ikuhara, Phys. Rev. B **68**, 085110 (2003).
[26] P. W. Peacock and J. Robertson, Appl. Phys. Lett. **83**, 2025 (2003).
[27] G. Lucovsky, J. Vac. Sci. Technol. **19**, 456 (1981).
[28] K. Kimoto, Y. Matsui, T. Nabatame, T. Yasuda, T. Mizoguchi, I. Tanaka, and A. Toriumi, Appl. Phys. Lett. **83**, 4306 (2003).
[29] A. G. Aberle, S. Glunz, and W. Warta, J. Appl. Phys. **71**, 4422 (1992).
[30] R. Hezel and R. Schorner, J. Appl. Phys. **52**, 3076 (1981).
[31] I. Martin, M. Vetter, M. Garin, A. Orpella, C. Voz, J. Puigdollers, and R. Alcubilla, J. Appl. Phys. **98**, 114912 (2005).
[32] M. J. Kerr and A. Cuevas, Semicond. Sci. Technol. **17**, 166 (2002).
[33] M. J. Kerr and A. Cuevas, Semicond. Sci. Technol. **17**, 35 (2002).
[34] S. W. Glunz, D. Biro, S. Rein, and W. Warta, J. Appl. Phys. **86**, 683 (1999).
[35] S. Dauwe, L. Mittelstadt, A. Metz, and R. Hezel, Prog. Photovoltaics **10**, 271 (2002).
[36] R. B. M. Girisch, R. P. Mertens, and R. F. Dekeersmaecker, IEEE Trans. Electron Devices **35**, 203 (1988).
[37] B. Kuhlmann, A. G. Aberle, and R. Hezel, Proceedings of the 13th European PVSEC, Nice, France (Stephens Bredford, UK, 1995), p. 1209.
[38] J. R. Elmiger, R. Schieck, and M. Kunst, J. Vac. Sci. Technol. A **15**, 2418 (1997).
[39] R. Hezel and K. Jaeger, J. Electrochem. Soc. **136**, 518 (1989).
[40] S. Dauwe, J. Schmidt, A. Metz, and R. Hezel, Proceedings of the 29th IEEE Photovoltaic Specialist Conference, New Orleans (IEEE, Piscataway, NJ, 2002), p. 162.
[41] G. Lucovsky, Y. Wu, H. Niimi, V. Misra, and J. C. Phillips, Appl. Phys. Lett. **74**, 2005 (1999).
[42] M. Garin, U. Rau, W. Brendle, I. Martin, and R. Alcubilla, J. Appl. Phys. **98**, 093711 (2005).
[43] S. Olibet, E. Vallat-Sauvain, and C. Ballif, Phys. Rev. B **76**, 035326 (2007).
[44] J. J. H. Gielis, B. Hoex, M. C. M. van de Sanden, and W. M. M. Kessels, J. Appl. Phys. **104**, 073701 (2008).
[45] E. H. Nicollian and A. Goetzberger, Bell Syst. Tech. J. **46**, 1055 (1967).
[46] I. S. Jeon, J. Park, D. Eom, C. S. Hwang, H. J. Kim, C. J. Park, H. Y. Cho, J. H. Lee, N. I. Lee, and H. K. Kang, Jpn. J. Appl. Phys., Part 1 **42**, 1222 (2003).
[47] C. T. Kirk, Phys. Rev. B **38**, 1255 (1988).
[48] G. S. Higashi and C. G. Fleming, Appl. Phys. Lett. **55**, 1963 (1989).
[49] D. G. Park, H. J. Cho, K. Y. Lim, C. Lim, I. S. Yeo, J. S. Roh, and J. W. Park, J. Appl. Phys. **89**, 6275 (2001).
[50] A. Chin, Y. H. Wu, S. B. Chen, C. C. Liao, and W. J. Chen, Proceedings of the VLSI Symposium, Honolulu (IEEE, Piscataway, NJ, 2000), p. 16.
[51] L. Manchanda, M. D. Morris, M. L. Green, R. B. van Dover, F. Klemens, T. W. Sorsch, P. J. Silverman, G. Wilk, B. Busch, and S. Aravamudhan, Microelectron. Eng. **59**, 351 (2001).
[52] S. Duenas, H. Castan, H. Garcia, A. de Castro, L. Bailon, K. Kukli, A. Aidla, J. Aarik, H. Mandar, T. Uustare, J. Lu, and A. Harsta, J. Appl. Phys. **99**, 054902 (2006).
[53] L. Truong, Y. G. Fedorenko, V. V. Afanasev, and A. Stesmans, Microelectron. Reliab. **45**, 823 (2005).
[54] M. Cho, H. B. Park, J. Park, S. W. Lee, C. S. Hwang, J. Jeong, H. S. Kang, and Y. W. Kim, J. Electrochem. Soc. **152**, F49 (2005).
[55] M. Shahjahan, T. Okada, K. Sawada, and M. Ishida, Jpn. J. Appl. Phys. **43**, 5404 (2004).
[56] J. Buckley, B. De Salvo, D. Deleruyelle, M. Gely, G. Nicotra, S. Lombardo, J. F. Damlencourt, P. Hollinger, F. Martin, and S. Deleonibus, Microelectron. Eng. **80**, 210 (2005).